Astronomy & Astrophysics manuscript no. aanda
December 9, 2020

Pulsar Scintillation Studies with LOFAR

Author1[1,⋆] author2[2]

[1] Fakultät für Physik, Universität Bielefeld, Postfach 100131, 33501 Bielefeld, Germany
e-mail: *@physik.uni-bielefeld.de
[2] Max-Planck-Institut für Radioastronomie, Auf dem Hügel 69, 53121 Bonn, Germany

Received **; accepted **

ABSTRACT

Context. extending interstellar medium studies to lower frequency band
Aims. we aim to study the interstellar propagation effect and the interstellar structures based on pulsar scintillation and DM
Methods. We observed * brighter pulsars with the LOw Frequency ARray (LOFAR) (DE601, DE602...) ** at 110-180 MHz.
Results. scintiles, arc , DM

Key words. interstellar medium – pulsar scintillation – DM

1. Introduction

The radio signal from a pulsar is perturbed by refractive index fluctuation in an turbulent medium, which will cause a a random phase of each ray. The interference between these scattered rays and also the relative motion of the pulsar, scattering material and the observer result in a modulation of the pulse intensity as a function of frequency, time and position of the observer plane which is called intersteller scintillation (ISS). The two branches of ISS are diffractive interstellar scintillation (DISS) caused by the samall spatial density fluctuations ($10^6 - 10^8$ m) and refractive interstllar scintillation caused by large-scale inhomogeneities ($10^{10} - 10^{12}$ m) in the interstellar medium (IISM), which remains distinct in the strong scattering where the DISS parameteres are modulated by RISS. A good review of ISS theory and phenomena may found in Narayan (1992).

Recently, scintillation arc has been confirmed in secondary spectrum that is the power spectrum of the dynamic spectrum (Stinebring et al.2001). These scinticlation arcs, which are clodely realted to multiple imageing abd frequently observed 'criss-cross' sloping bands, result from interference between rays in a central core and rays from an extended scattering disc (M.A.Walker et al.2004, Cordes et al.2006). The curvature of arcs in the secondary spectrum depends on the distance to the scattering region and the velocity of the line-of-sight with respect to the medium.

In this work, we present the first puslar scintillation studies with the LOw Frequency ARray (LOFAR). The key point of studying pulsar scintillation at low frequency is that lower frequencies probe larger scattering angles ($\theta_{sca} \sim \lambda^2$). Furthermore, larger scattering angle probe larger time delay ($\tau \sim \lambda^4$). Time delay is the geometric time delay of the scattered rays compared to the line of sight. In practice so far, scintillation arcs have almost exclusively been probed at delays of a few microseconds at most, with an exceptional record of 1 ms. The biggest advantage of studying pulsar scintillation is that we are able to study more wider refracting sheets.

⋆ and

2. Observations and data processing

2.1. Observations

Our analysis is based on data from six German stations (van Haarlem et al. 2013), namely the stations in Effelsberg (telescope identifier DE601), Tautenburg (DE603) and Jülich (DE605), one French station in Nançay named FR606 of the International LOFAR Telescope used in stand alone mode and LOFAR core from time to time in the frequency range110-188 MHz (see Table 2).

Our pulsar processing pipeline was based on DSPSR2(van Straten & Bailes 2011) which coherently dedispersed the data, folded the resulting time series at the period of the pulsar, and created subintegrations of 10 s. Subsequently, observations were written out in PSRCHIVE3 (Hotan et al. 2004) format.

2.2. data processing

2.2.1. radio-frequency interference (RFI)

The RFI cleaning program iterative_cleaner[1] is a modification of the surgical cleaner included in the coastguard pipeline (Lazarus et al.(2016)).

Two major changes were made: 1. the cleaner uses an iterative approach for the template profile. This helps when the pulsar is masked by RFI in the original template profile. 2. the detrending algorithm was removed. This feature may be reintroduced with different default parameters.

2.2.2. DM time series

In order to determine highly precise and reliable DM values, we used a frequency-resolved template. To create the template we combined several longer observations with Higher S/N taken with DE601 for each pulsar. These observations were averaged in time and summed to total intensity, providing a frequency-

[1] https://github.com/larskuenkel/iterative_cleaner

Pulsar	DM	GL	GB	XX	YY	ZZ
0332+5434	26.7641	145.00	-1.22	0.57	9.32	-0.02
0814+7429	5.75066	140.00	31.62	0.24	8.78	0.23
0826+2637	19.47633	196.96	31.74	-0.08	8.76	0.17
0837+0610	12.8640	219.72	26.27	-0.11	8.63	0.08
0953+0755	2.96927	228.91	43.70	-0.14	8.62	0.18
1136+1551	4.84066	241.90	69.20	-0.11	8.56	0.33
1239+2453	9.25159	252.45	86.54	-0.05	8.52	0.84
1509+5531	19.6191	91.33	52.29	1.28	8.53	1.66
1921+2153	12.44399	55.78	3.50	0.25	8.33	0.02
2018+2839	14.1977	68.10	-3.98	0.91	8.14	-0.07
2022+2854	24.63109	68.86	-4.67	1.95	7.75	-0.17
2022+5154	22.54968	87.86	8.38	1.78	8.43	0.26
2219+4754	43.4975	98.38	-7.60	2.34	8.85	-0.32

Table 1: The properties of Puslars

Table 2: THE OBSERVING PARAMETERS

Pulsar (PSR J)	model	station	length (hours)	Δ_f (kHz)	δt (s)	Number
0332+5434	Scintillation	FR606	1	0.3	10	1
0814+7429	Scintillation	DE601	1	10		
		DE603	1	10		
		DE604	1	10		
	Timing	DE601	1	10		
0826+2637	Scintillation	Core	0.5	0.98	5	1
0837+0610	Scintillation	DE601	1	10		
		DE603	1	10		
		DE604	1	10		
	Timing	DE601	1	10		
0953+0755	Scintillation	DE601	1	10		
		DE603	1	10		
		DE604	1	10		
	Timing	DE601	1	10		
1136+1551	Scintillation	DE601	1	10		
		DE603	1	10		
		DE604	1	10		
	Timing	DE601	1	10		
1239+2453	Scintillation	DE603	1	10	10	1
1509+5531	Scintillation	FR606	1	10		
1921+2153	Scintillation	DE601	1	10		
		DE603	1	10		
		DE604	1	10		
	Timing	DE601	1	10		
2018+2839	Scintillation	FR606	1	10		
2022+2854	Scintillation	Core	0.5	10		1
2022+5154	Scintillation	Core	0.5	10		1
2219+4754	Scintillation	Core	0.5	10		1

resolved pulse profile with a S/N a few times that of the typical observation.

2.2.3. Scintillation parameters

In this work, we use psrchive command 'dynamic spectrum' or 'Psrflux' to create our initial dynamic spectrum. After the program loads the dynamic spectrum, trends in both the frequency direction as well as the time direction have to removed from the dynamic spectrum. After that step the mean value of the dynamic spectrum has to be subtracted from the dynamic spectrum as well.

Using the dynamic spectrum, one can estimate the decorrelation bandwidth B_{iss}, decorrelation (diffractive) time-scale τ_{iss} by computing a two-dimensional ACF of S(f, t) in frequency and time lags (1):

$$\rho(\nu, \tau) = < S(f, t)S(f + \nu, t + \tau) > . \quad (1)$$

where v and τ are the frequency and time lags, respectively.

Following Reardon et al. (2019); Coles et al. (2010, 2005), To calculate this we remove the mean, then pad each segment with an equal length of zeroes in both dimensions, perform a 2-D FFT on the zero-padded segment, take the squared magnitude of the result, and perform an inverse 2-D FFT. We then perform

a emcee fit to $C(\tau, 0)$ and $C(0, \Delta\nu)$ to obtain $\tau_{\rm d}$ and $\Delta\nu_{\rm d}$ respectively. First we fit $C(\tau, 0)$ with

$$C(\tau,0) = A\exp\left(-\left|\frac{\tau}{\tau_{\rm d}}\right|^{\frac{5}{3}}\right)\Lambda(\tau, T_{\rm obs}), \text{for } \tau > 0 \quad (2)$$
$$C(0,0) = W + A.$$

where $T_{\rm obs}$ is the length of each observation, $\Lambda(\tau, T_{\rm obs})$ is the triangle function of length $\pm T_{\rm obs}$, and W is the variance noise spike. We then fit $C(0, \delta\nu)$ with

$$C(0,\delta\nu) = A\exp\left(-\left|\frac{\delta\nu}{\Delta\nu_{\rm d}/\ln 2}\right|\right)\Lambda(\delta\nu, B), \text{for } \delta\nu > 0 \quad (3)$$
$$C(0,0) = W + A$$

to obtain $\Delta\nu_{\rm d}$, where B is the frequency band of the dynamic spectrum. Here, we assume that refractive variations are negligible over the length of each observation (usually 2 hours).

The uncertainty of the scintillation parameters consists of the uncertainty coming from the fitting procedure and the statistical error due to the finite number of scintles (see Equation. 4). Finally, The two uncertainty sources are added quadratically to get the error.

$$\sigma_{est} = [f_d * \frac{B_{dyn}t_{dyn}}{\nu_d\tau_d}]^{-0.5}. \quad (4)$$

Here, B_{dyn} is the frequency band of dynamic spectrum, t_{dyn} is the length of the dynamic spectrum, σ_{est} is the statistical fractional uncertainty and f_d is the filling factor.

In order to obtain the parameter called drift rate, we also use two-D Gaussian function to fit the ACF with Least squares to determine the optimal solutions. and also the secondary spectrum is the Fourier transform fo the ACF, whcih makes the drift rate become a probe of the asymmetry the scintillation arc.

3. scintillation census

13 slow pulsars have been confirmed with scintillation effect at LOFAR, including 7 scintillation arc sources (Figure 1). A quantitative measurement of the strength of scattering is the parameter U (Eq. 5) which is defined as the ratio of the Fresnel scale to the coherence scale. These 13 slow pulsars are both in strong scattering ($U > 1$).

$$u \approx (\frac{2\nu}{\Delta\nu_d})^{0.5} \quad (5)$$

Then talk about the refractive scintilltion. First give an equation to calculate the refractive scintilltion time-scale (τ_{ref}). Absolutly, the observing length of each epoch is shorter than the τ_{ref}, which means our measurements didn't remove the effect from refractive scintillation. Then, for these pulsars with long-term-monitoring, we are able to remove refractive scintillation.

Also, we could discuss the scattering region s_r from Eq. 6

$$s_r/r_F = \sqrt{\nu/\Delta\nu_d}, \quad (6)$$

wheren $r_F = \sqrt{De/k}$ is the 'Fresnel scale'. I suspect the scattering region should be AU-scale.

3.1. Kolmogorov spectrum

This high sensitivity and the fact that even a narrow frequency range can achieve numerous scintles, allows thorough and self-consistent statistical analyses of scintillation scaling laws. In most cases of the previous works, the frequency scaling factor was calculated by the measured scintillation bandwidths at different epochs. Thus, the measured frequency scaling factor is modulated by refractive scintillation. Here, we report our independent scintillation scaling factor with Lofar data set. We obtain the scintillation bandwidth with 10 MHz frequency band, which makes we have seven measures of scintillation bandwidth at different frequency range for a single archive (Figure 2). Then, based on the scintillation bandwidth that were measured from a single archive, we are able to get the frquency scaling facto). The frequency scaling factor of B0329+54, B0809+74, B0823+26, B1919+21 is consistent with the prediction of the kolmogorov spectrum. We note that the frequency scaling factor also has found variation over time which suggests the ISM is not extremely stable.? Although the discrepancy between our results and previous ones can be ignored for some pulsars because of refractive scintilltion, the huge gap between our measures and the parameters of B1508+55 of Huguenin et al. (1969) is still a puzzle. This could be the different ISM structure in the line of sight, after all, our observation is made at 50 years later.

3.2. scintillation bandwidth vs DM

To study the dependence of ISS and DM we have scintillation bandwidth as a function of DM (Figure 3).

The thin screen theory predicts that

$$\nu_d \sim DM^{-2}F^4 \quad (7)$$

Wolszczan (1977) found that the this two parameters conform to the theoretical slope of -2 remarkably well. However, Balasubramanian & Krishnamohan (1985) found that there are three pulsars (PSR B0628-28, B0833-45 and B1933+16) that seem to deviate significantly from the general trend of the other points. Their best fit is given by $f_v(kHz) \propto DM^{-1.79\pm0.14}$ without considering those unusually points. It is known that the Gum nebula causes excessive scattering in the case of Vela pulsar (e.g. Backer 1974).

The solid line represents the best fit to these data by means of the least squares method.

De-correlation bandwidth of ten pulsars plotted as a function of dispersion measure. The values measure at both 145MHz are well correlated with dispersion measure, except B1133+16.

3.3. scintillation velocity vs pulsar proper motion

In the most case, the relative motion of the observe with respect to the scintillation pattern is a combination of the transverse motions of the pulsar and observer, as well as the motion of the scattering medium. This makes scintillation speed as a tool for measuring the pulsar proper motion. Some authors found good agreement between ISS speeds and proper motion speed (Lyne & Smith 1982; Cordes 1986; Gupta et al. 1994; Gupta 1995). It also has been reported that there is systematic bias in theta ISS speeds trend to be lower than proper motion speeds (Harrison & Lyne 1993) and the scintillation velocity of a local millisecond pulsar PSR J0437-4715 is two times larger than proper motion speed because of scattering from local bubble (Gothoskar & Gupta 2000).

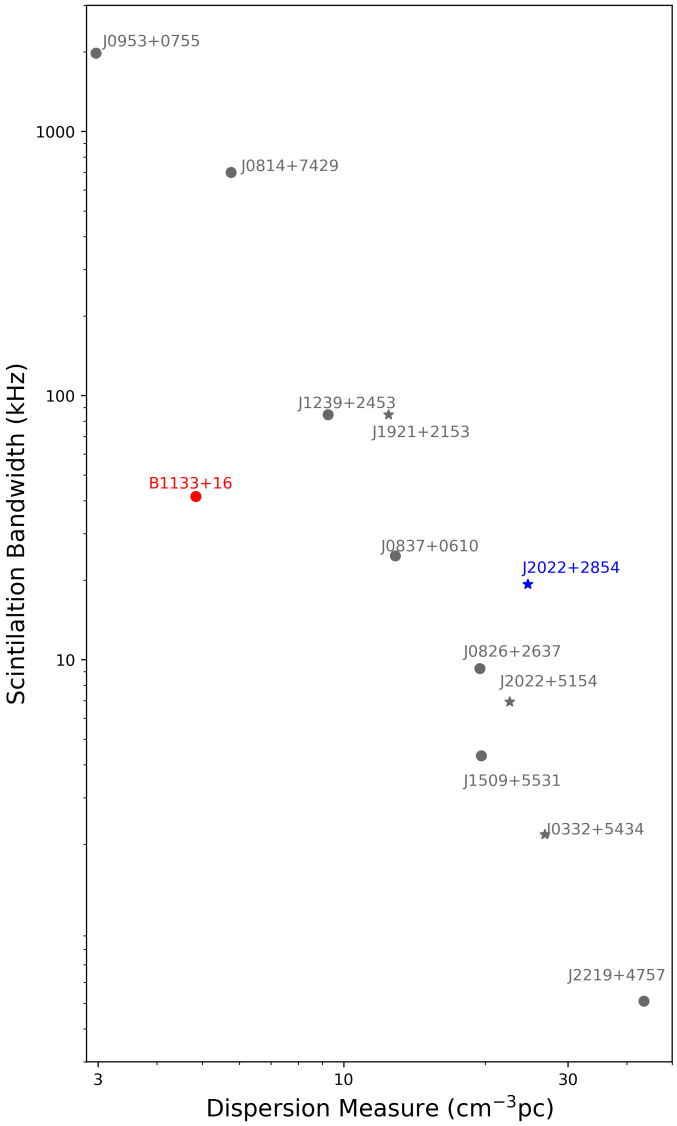

Fig. 3: Scintillation bandwdith Vs DM. The filled circles indicate the pulsars with high galactic latitude (b > 30) and low latitude sources (b <10).

Here we study the correlation between scintillation velocity and proper motion velocity based on our results. We measure the scintillation velocity with the mean value of the scintillation parameters to eliminate refractive effect.

3.4. scintillation arc curvature

Scintillation arc were first found by Stinebring et al. (2001), also used to measure the location of phase changing screen. Here, we report that some pulsars can be observed scintillation arc, which is J0814+7429 (first time), J0826+2637, J0837+0610, J0953+0755, J1136+1551, J1239+2453, J1921+2153, J2018+2839 (other person already also found, but this have not been published) J2022+5154 and J2219+4757 (first time). Scintillation arc at Lofar frequency range are usually diffuse and thick (Stinebring et al. 2019), which makes measuring the arc curvature is a pain for some pulsars.

Stinebring et al. (2001) detected arc from J0826+2637, J1136+1551 and J0837+0610 at 430 MHz. We measure the arc curvature based on hough transform. The arc curvature of J0826+2637 at 140-150 MHz is 2.27 ± 0.27 us/mhz^2 Fig. 4. The arc curvature of J1136+1551 at 139-149 MHz is 0.36170 ± 0.02553 us/mhz^2. The arc curvature of J0837+0610 at 140-150 MHz is 2.90 ± 0.34 us/mhz^2 (Hill et al. 2005: 0.47±0.03 s^3 at 327 MHz).

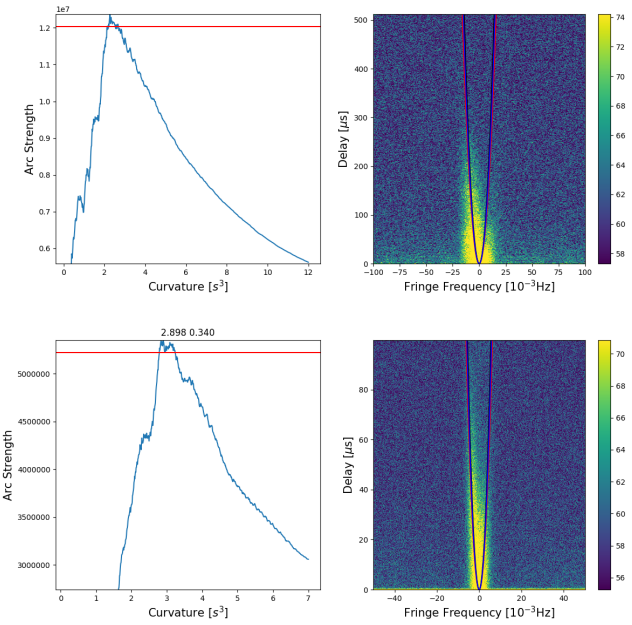

Fig. 4: Hought Transform of B0823+26(top) and J0837+0610(bottom).

4. scintillation long term monitoring

scintillation parameters, delta DM, frequency scaling of the scintillation, scintillation arcs and its asymmetry in the function of MJD.

4.1. the variation of the asymmetry of scintillation arc

The title of ACF is related to the asymmetry of scintilltion arc from J1136+1551. We can see a clear varation of the title of ACF. What can cause this kind of variation? I mean at some epochs, the right side of arc is stronger, sometimes, left side of arc is stronger? If this is related to the motion of IISM, then why does it change?

4.2. scintillation parameters long term variations (refractive)

For now, we have four pulsars with long scintillation monitoring. Unfortunately, two of them (J0953+0755, J0814+7429) have calibration errors of normal frequency resolution GLOW data set, are not suitable for pulsar timing studies (DM, particularly). The time series of scintillation parameters and δ DM (if possible) are shown in Fig The quasi-periodic varaition of scintillation paramters could be caused by refractive scintilltion, for example: J1136+1551 during MJD: 57100-57200. Then what is the reason that cause 'vally-like' varaition in scintilltion parameters, for example J1136+1551 during MJD: 57450 - 57500.

4.3. Δ DM annual variation

DM could have annual variation and monotonically increasing or decreasing trends (e.g. Jones et al. 2017). Here, we report the ΔDM of J0837+0610 represents annual and linear variations (Figure 6) (Is this the first normal pulsar with annual variation?)

Following (e.g. Jones et al. 2017), we have plotted the pulsar trajectories through the ISM as seen from Earth. For this, we assumed that all of the free electrons along the LOS are sitting in a stationary phase screen located halfway between the Earth and the pulsar. The trajectories are the projected motions of the pulsar as seen on this phase screen. Using proper motion and distance estimates with errors from "PSRCAT", the transverse velocity can be calculated and used to track the pulsar's trajectory in the sky. These trajectory maps can be useful in isolating features in the ISM as well as visualizing trends in the DM time series. The ΔDM shows decreasing linear trend, but with two different slope rates. and the pulsar trajectories show clearly annual variations, which makes the earth motion could be the reason of ΔDM annual variation.

4.4. the annual variation of scintillation time-scale

The spatial scale of the diffractive scattering, $s_{\rm d}$ is defined as the transverse separation where incident waves have a 1 radian rms difference in phase, which can be calaulated from $\nu_{\rm d}$ (Cordes & Rickett 1998)

$$s_{\rm d} = \frac{1}{\nu}\left(\frac{cD\nu_{\rm d}}{4\pi C_1}\right)^{1/2} W_{\rm DISS} \tag{8}$$

where ν is the frequency in the unit of GHz, c is the speed of light, D is the distance to the pulsar in the unit of kpc, $\nu_{\rm d}$ is the diffraction or scintillation bandwdith in the unit of MHz. Since you do observe a clear arc you know that the scintillations are dominated by a thin sceen. For a thin screen under the kolmogorov case, C_1 is 0.96, and $W_{\rm DISS} = [2(D-D_s)/D_s]^{1/2} = [2(1/s-1)]^{1/2}$, where s is position of scattering screen (s = 0 at the pulsar, s = 1 at the Earth)

For solitary pulsars, the effective transverse line-of-sight velocity $V_{\rm eff}(s)$ through the scattering medium at position s, which is a linear combination of the pulsar, Earth, and IISM velocities:

$$V_{\rm eff}(s) = (1-s)V_{\rm p} + sV_{\rm E} - V_{\rm IISM}(s) \tag{9}$$

The transverse velocity of the pulsar $V_{\rm p}$ has components $v_{\rm p,\parallel}$ along the RA, and $v_{\rm p,\perp}$ perpendicular to this in DEC.

4.4.1. Isotropic IISM

The effective velocity is simply given by

$$V_{\rm eff}(s) = \sqrt{v_{\parallel}(s)^2 + v_{\perp}(s)^2}. \tag{10}$$

The scintillation timescale can be predicted by ($V_{\rm los} = V_{\rm eff}/s$)

$$\begin{aligned}\tau_{\rm d} &= \frac{s_{\rm d}}{V_{\rm los}} \\ &= \frac{s_{\rm d}s}{V_{\rm eff}} \\ &= \frac{s_{\rm d}s}{\sqrt{v_{\parallel}(s)^2 + v_{\perp}(s)^2}}\end{aligned} \tag{11}$$

So the most important parameter is the screen distance. I can estimate the spatial scale from the bandwidth, but it might be better to assume it is a constant and fit it. Then I need the Vism in RA and DEC. That's a 4 parameter fit, but the data have 5 degrees of freedom, so I can fit all those parameters.

4.4.2. Anisotropic IISM

We describe the anisotropy by two quantities, the axial ratio $A_{\rm R}$ and the orientation of the major axis $\psi_{\rm AR}$ of the inhomogeneities in the plasma density. The anisotropy effect the $V_{\rm eff}$. Rickett14 parametrised the quadratic coefficients in terms of $R = (A_R^2 - 1)/(A_R^2 + 1)$, which is bound between 0 and 1. If the orientation angle $\psi_{\rm AR}$ is defined clockwise from the RA, the from Rcikett et al.2014, the coefficients are

$$\begin{aligned}a &= \left[1 - R\cos\left(2\psi_{\rm AR}\right)\right] / \sqrt{1-R^2} \\ b &= \left[1 + R\cos\left(2\psi_{\rm AR}\right)\right] / \sqrt{1-R^2} \\ c &= -2R\sin\left(2\psi_{\rm AR}\right) / \sqrt{1-R^2}.\end{aligned} \tag{12}$$

Finally, we introduce a scaling factor κ to the model, which will account for any errors (for example an error in the pulsar distance D) in the calculation of $V_{\rm ISS}$ from the dynamic spectrum. Our final model for the effective velocity is then

$$V_{\rm eff}(s) = \kappa\sqrt{av_{\parallel}(s)^2 + bv_{\perp}(s)^2 + cv_{\parallel}(s)v_{\perp}(s)}, \tag{13}$$

The scintillation timescale can be predicted by

$$\begin{aligned}\tau_{\rm d} &= \frac{s_{\rm d}}{V_{\rm los}} \\ &= \frac{s_{\rm d}s}{V_{\rm eff}} \\ &= \frac{s_{\rm d}s}{\kappa\sqrt{av_{\parallel}(s)^2 + bv_{\perp}(s)^2 + cv_{\parallel}(s)v_{\perp}(s)}}\end{aligned} \tag{14}$$

If the scattering is anisotropic you'll also need the axial ratio and its orientation. That would make the fit impossible without using an estimate of the spatial scale from the bandwidth. However if you do that I would still recommend that you try estimating the spatial scale from all the bandwidth measurements altogether first, to minimize the effect of noise in the bandwidth estimation.

Another reason for being cautious about the bandwidth is that the bandwidth estimate depends on the phase gradient and you have some very clear phase gradients. However the timescale does not depend on the phase gradient. So some of that bandwidth noise could be real but due to the phase gradient not the spatial scale.

4.4.3. Fitting with J0814+7429

We fit the data with Markov chain Monte Carlo simulation (Fig 7, Fig 8).

4.5. compare the relationship between scintillation and DM (ESE)

The DM is the integrated column density of free electrons along the line of sight (LOS) to a pulsar:

$$DM = \int_a^b n_e(l)dl, \tag{15}$$

5. Conclusion

We are having more scintillation test observation new. Scintillation studies based on Lofar data are highly sensitive with nearby pulsars (DM < 30), it is a great prob of local bubble.

References

Backer, D. C. 1974, ApJ, 190, 667
Balasubramanian, V. & Krishnamohan, S. 1985, Journal of Astrophysics and Astronomy, 6, 35
Coles, W. A., McLaughlin, M. A., Rickett, B. J., Lyne, A. G., & Bhat, N. D. R. 2005, ApJ, 623, 392
Coles, W. A., Rickett, B. J., Gao, J. J., Hobbs, G., & Verbiest, J. P. W. 2010, ApJ, 717, 1206
Cordes, J. M. 1986, ApJ, 311, 183
Gothoskar, P. & Gupta, Y. 2000, ApJ, 531, 345
Gupta, Y. 1995, ApJ, 451, 717
Gupta, Y., Rickett, B. J., & Lyne, A. G. 1994, MNRAS, 269, 1035
Harrison, P. A. & Lyne, A. G. 1993, MNRAS, 265, 778
Huguenin, G. R., Taylor, J. H., & Jura, M. 1969, Astrophys. Lett., 4, 71
Jones, M. L., McLaughlin, M. A., Lam, M. T., et al. 2017, ApJ, 841, 125
Lyne, A. G. & Smith, F. G. 1982, Nature, 298, 825
Reardon, D. J., Coles, W. A., Hobbs, G., et al. 2019, MNRAS, 485, 4389
Stinebring, D. R., McLaughlin, M. A., Cordes, J. M., et al. 2001, ApJ, 549, L97
Stinebring, D. R., Rickett, B. J., & Koch Ocker, S. 2019, ApJ, 870, 82
Wolszczan, A. 1977, Acta Astron., 27, 127

Appendix A: Measure the pulse broadening delay

Here, the first thing I need to do is to develop some code to measure the pulse broadening time. Now I am trying to follow their work. What they used is is a clean-based method. Usually, the clean algorithm is designed for image area. The basic idea of this algorithm is that the image that we detected is a convolution of intrinsic image with the point spread function. If we know the point spread function, then we could reconstruct the intrinsic image from the dirty image. When this clean algorithm comes to pulse broadening area, the difficult is that we don't know the point spread function. The reason we don't know the point spread function is because we don't know the pulse broadening time. Following their work, what I could do is I could try different pulse broadening time to see which one gives a better result. To determine which one is the best, we have two parameters. The first one is to describe the asymmetry of the restored intrinsic pulse profile and the second one is to measure the pomposity of the residual in the final iteration. So for each pulse broadening time, we can have these two parameter. The third parameter is the sum of these two parameters. The corresponding value in the X-axis of the minimum of the third parameter is the best pulse broadening time. Here, the best pulse broadening time is about 4.5 ms. And the is the restored intrinsic pulse profile. let's compare this one and this one that I obtained from higher observation. I would say they look similar. So, for now, I already made more tests on my code. But unfortunately, it is not stable. For now, I would not do further research based on my code. I need to improve my code.

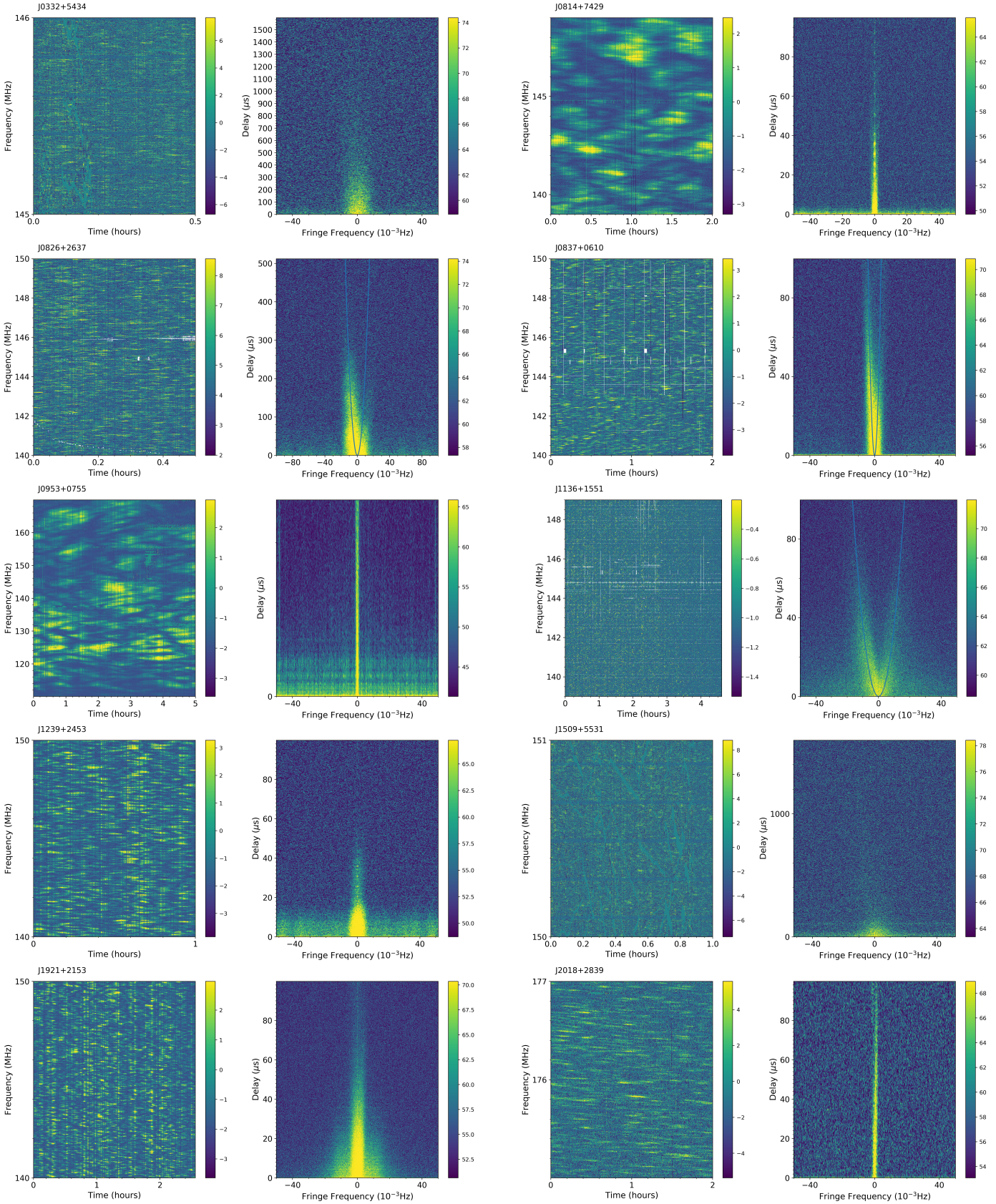

Fig. 1: Dynamic spectrum and Secondary spectrum from the Lofar observations

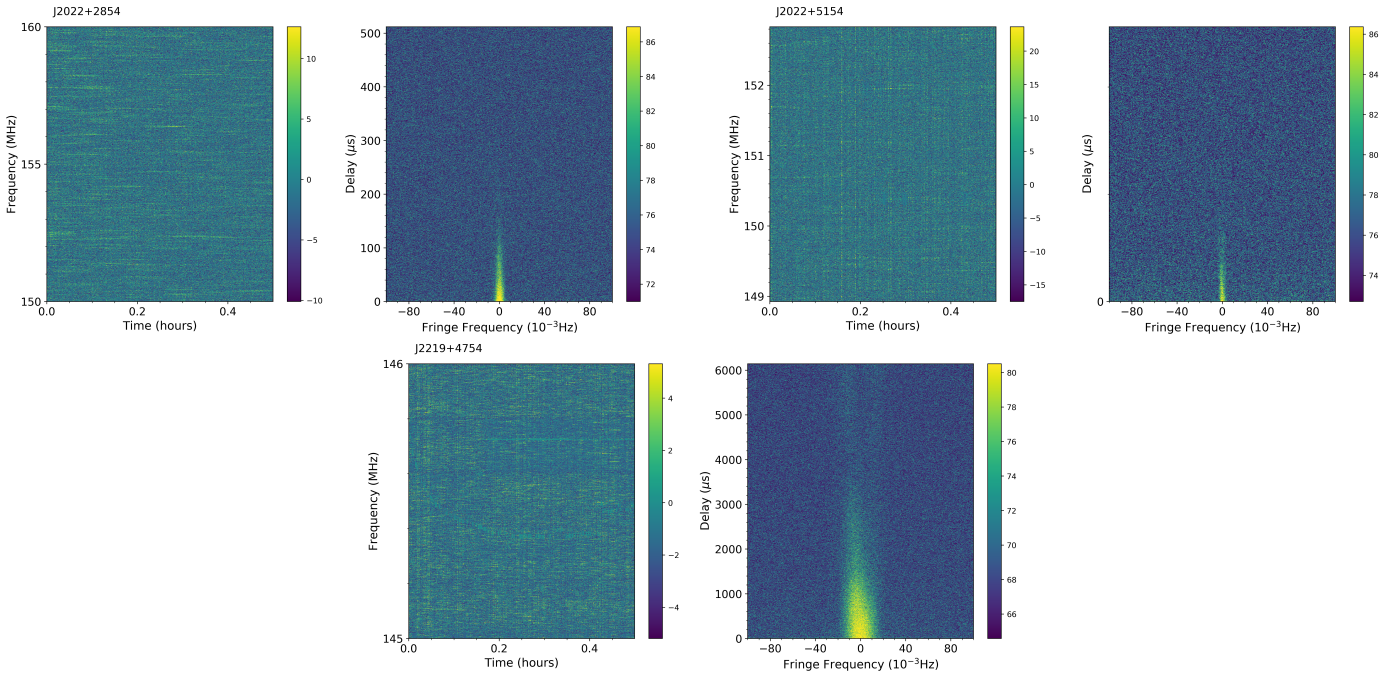

Fig. 1: continued

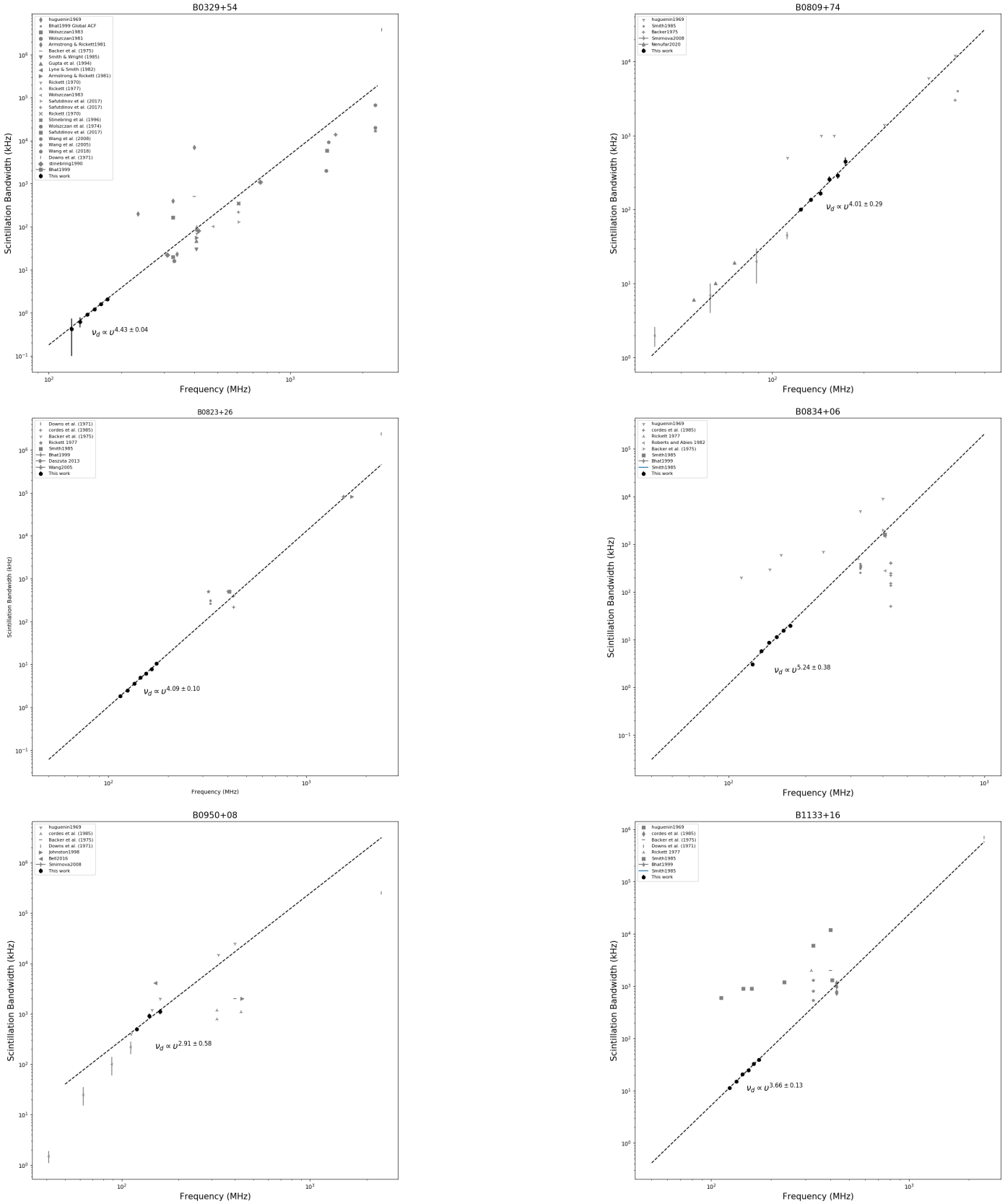

Fig. 2: Scintillation bandwidth as a function of observing frequency. The dash line represents the best fit of Lofar parameters.

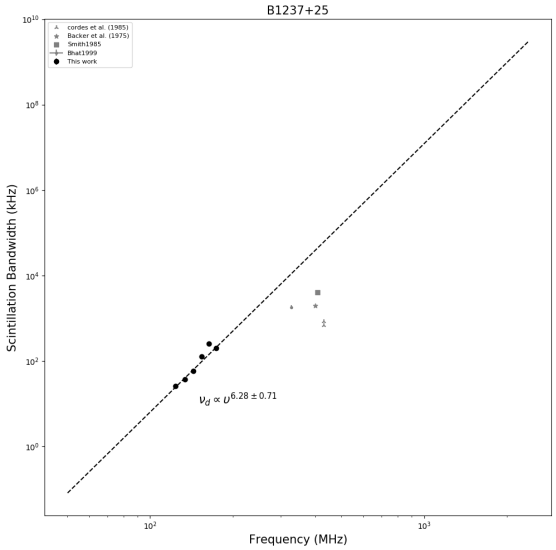

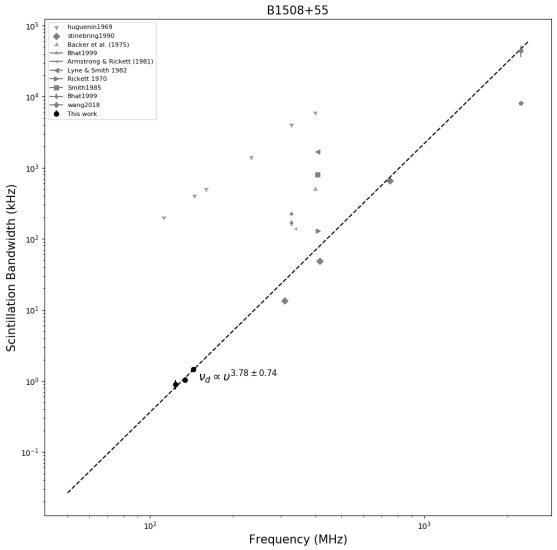

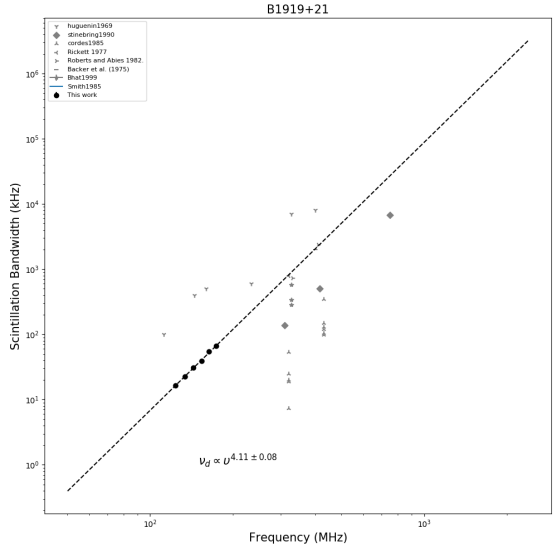

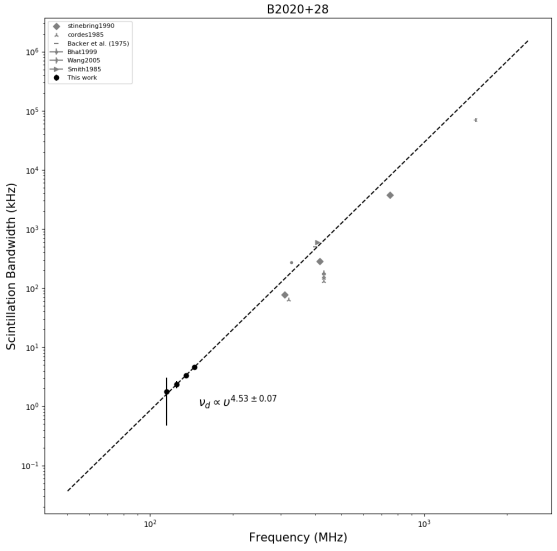

Fig. 2: continued

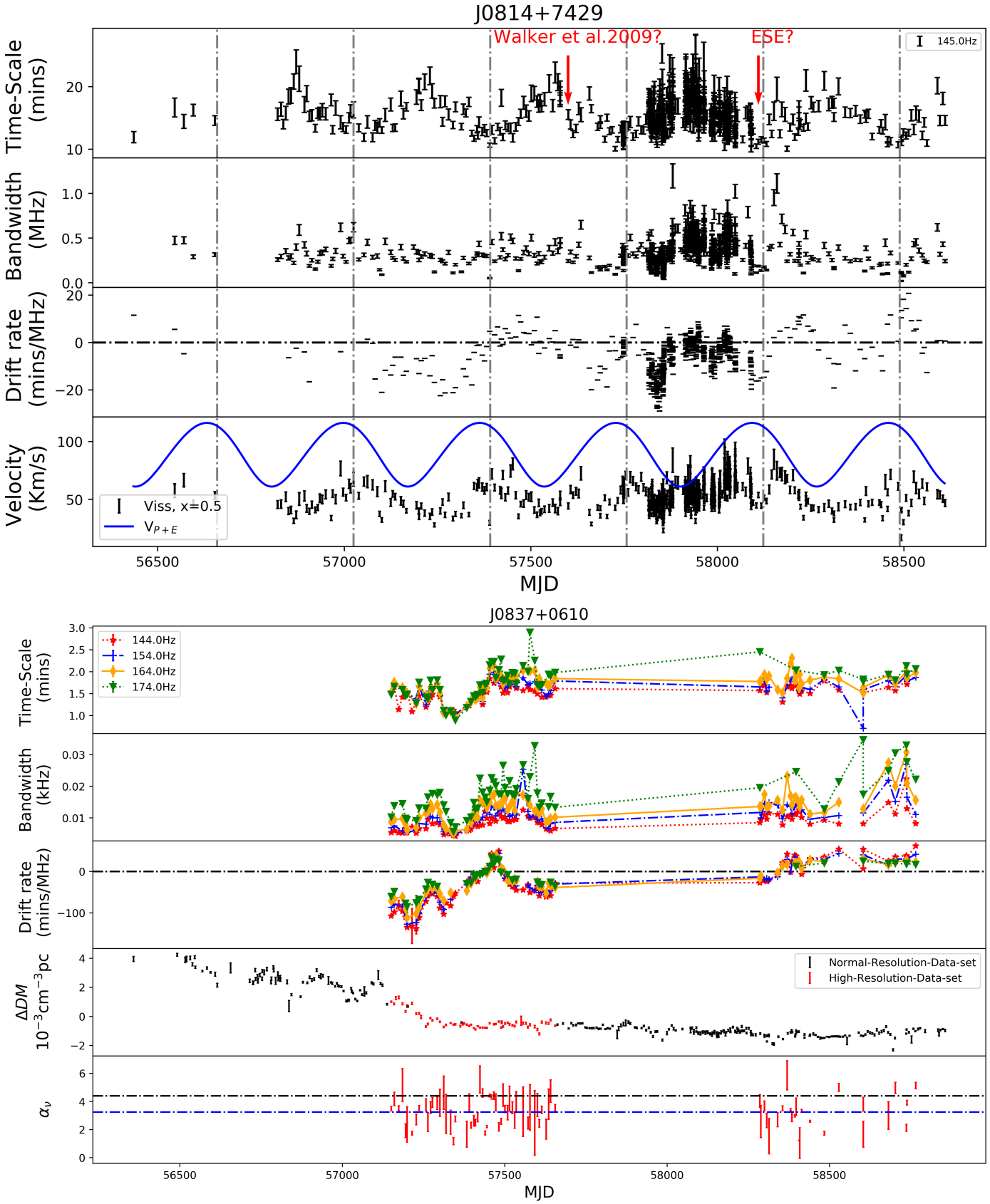

Fig. 5: Time series of scintillation (scintillation Bandwidth, timescale, drift rate and scintillation velocity), ΔDM and earth velocity. The uncertainties in the measurements indicate ± 1 σ error estimates, which include errors due to fitting and estimation errors due to the finite number of scintles at a given frequency range and a given epoch of observation.

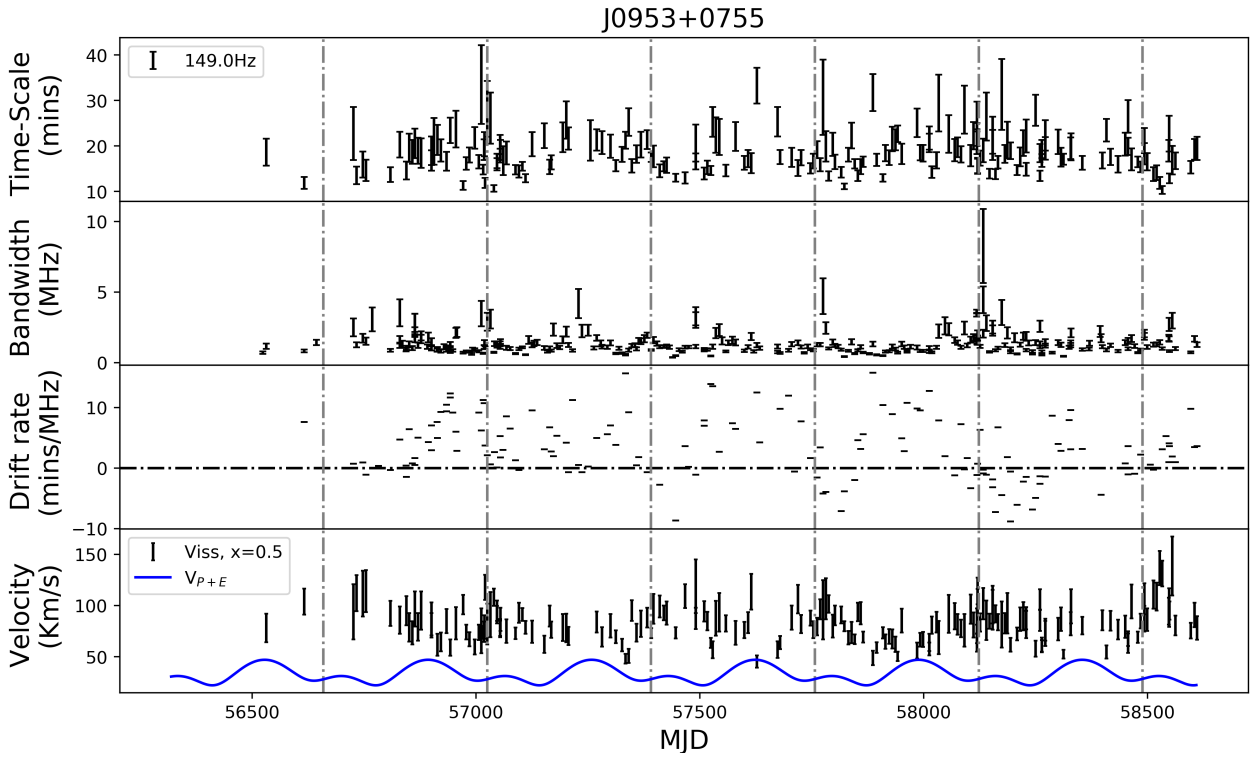

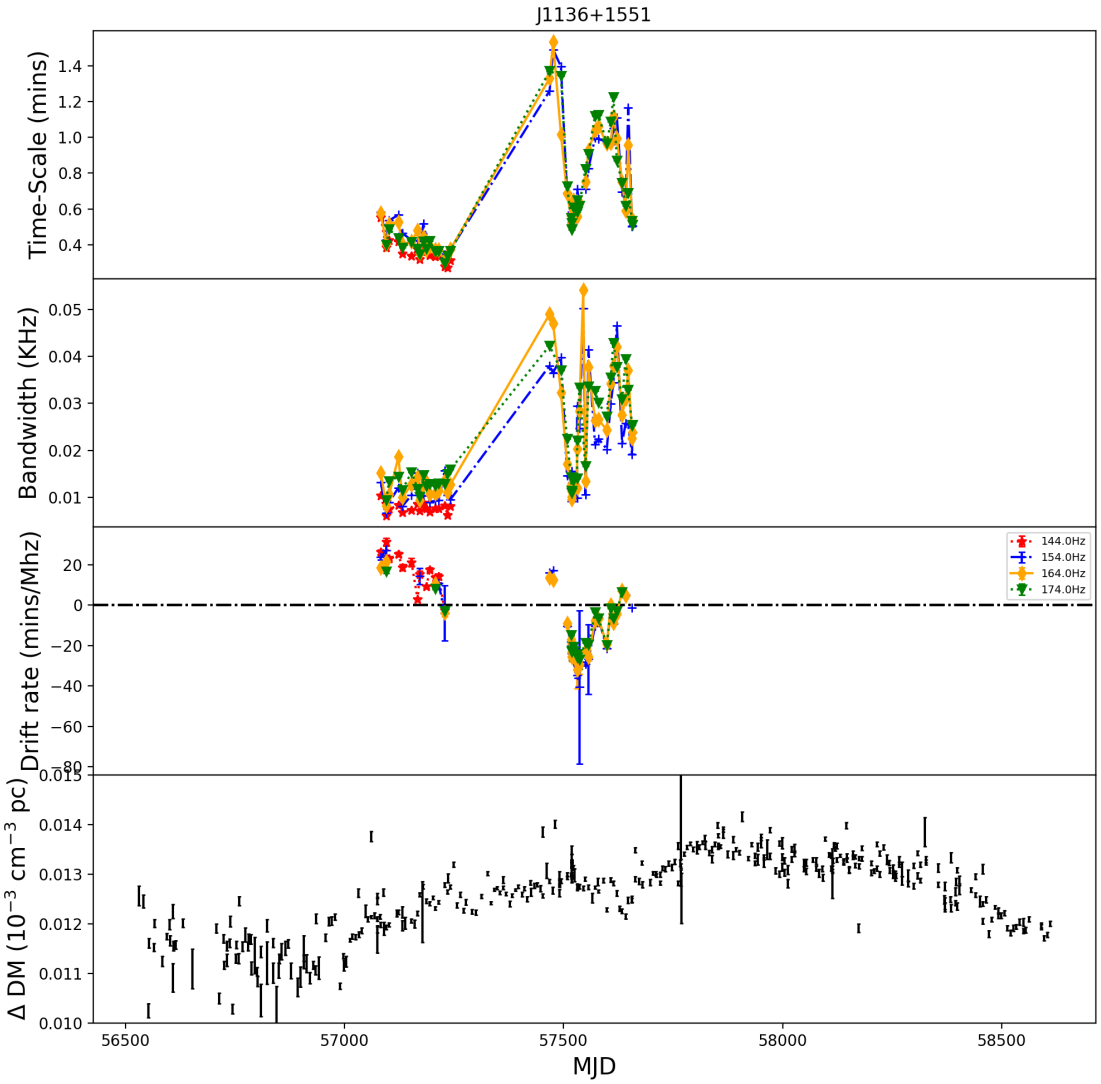

Fig. 5 (cont.): continued

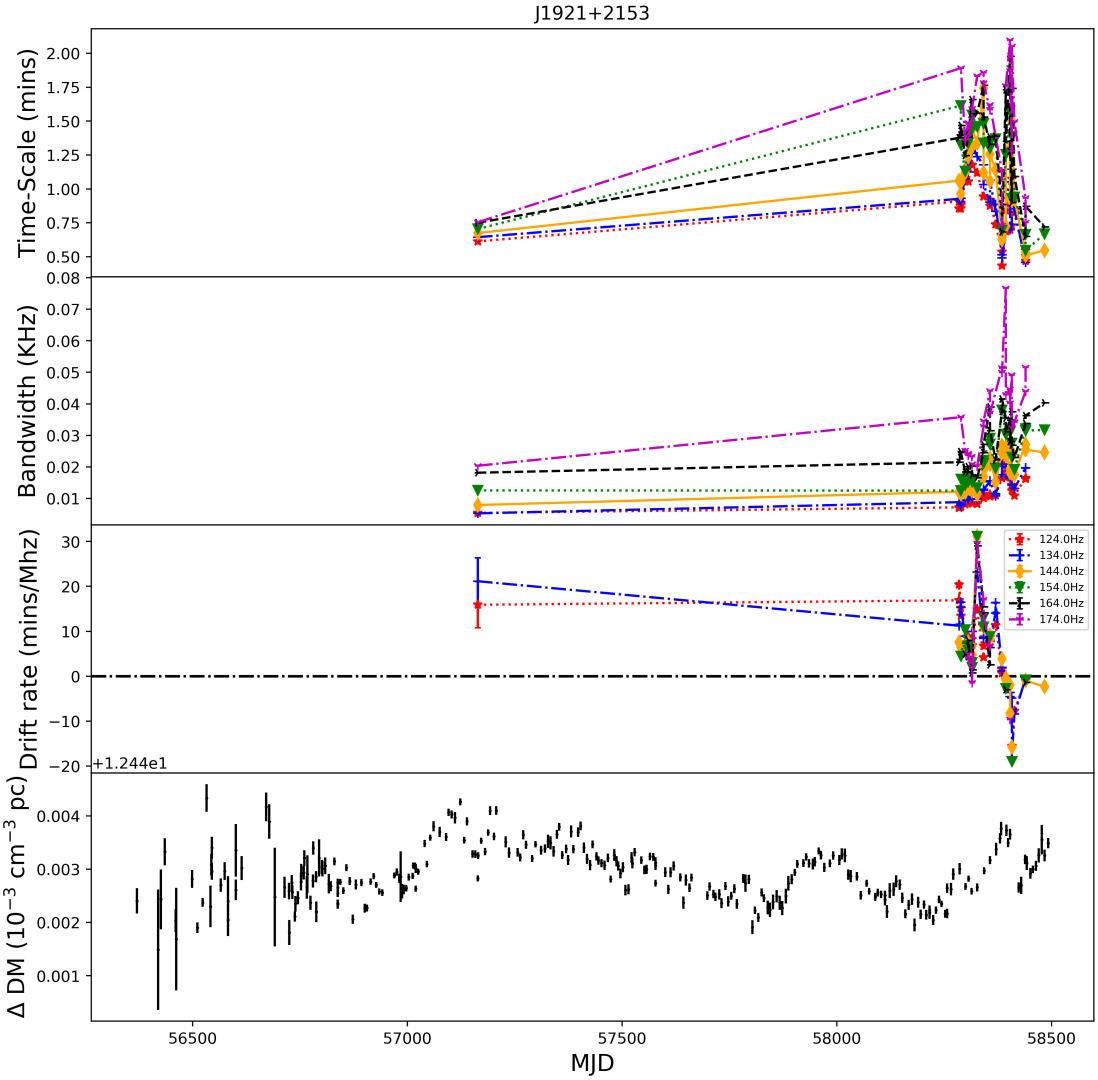

Fig. 5 (cont.): continued

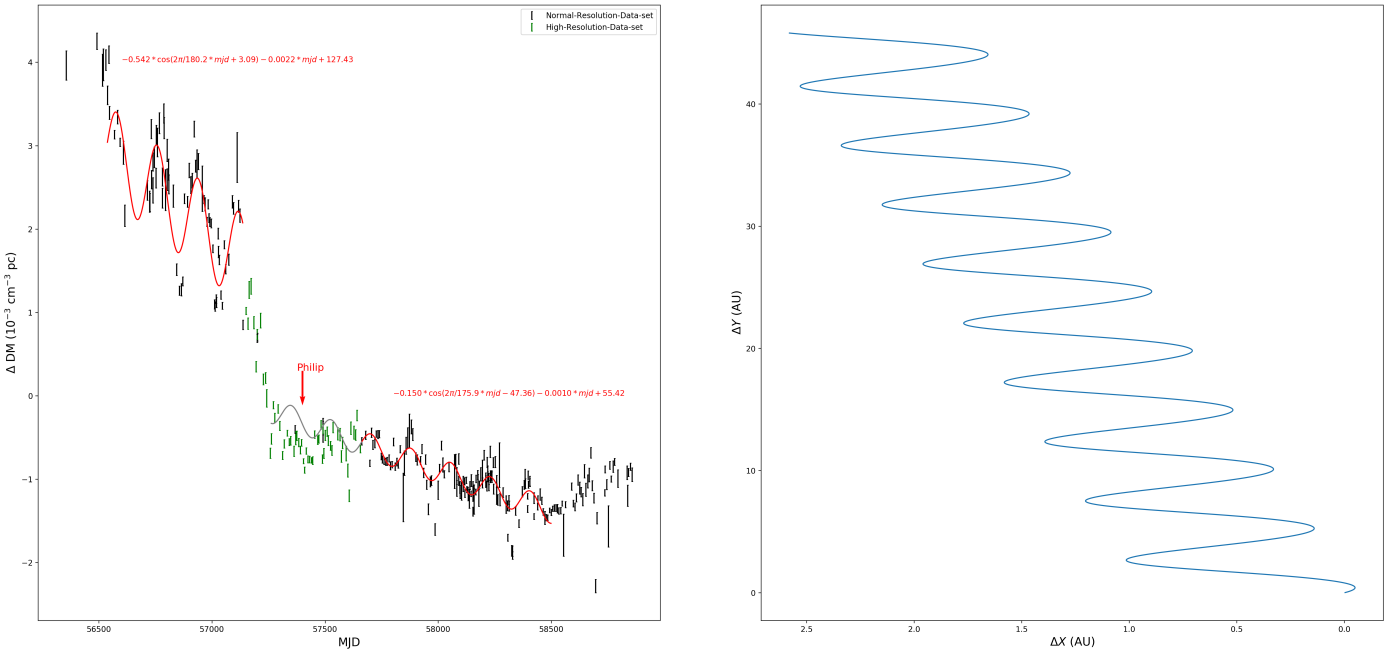

Fig. 6: The left panel shows the ΔDM time series of J0837+0610 with the best-fit function. The black and blue represent the data from normal and high frequency resolution, respectively. The gray line is the prediction value based on the fit for the second part of normal frequency resolution data. The right panel shows the pulsar trajectories of J0837+0610.

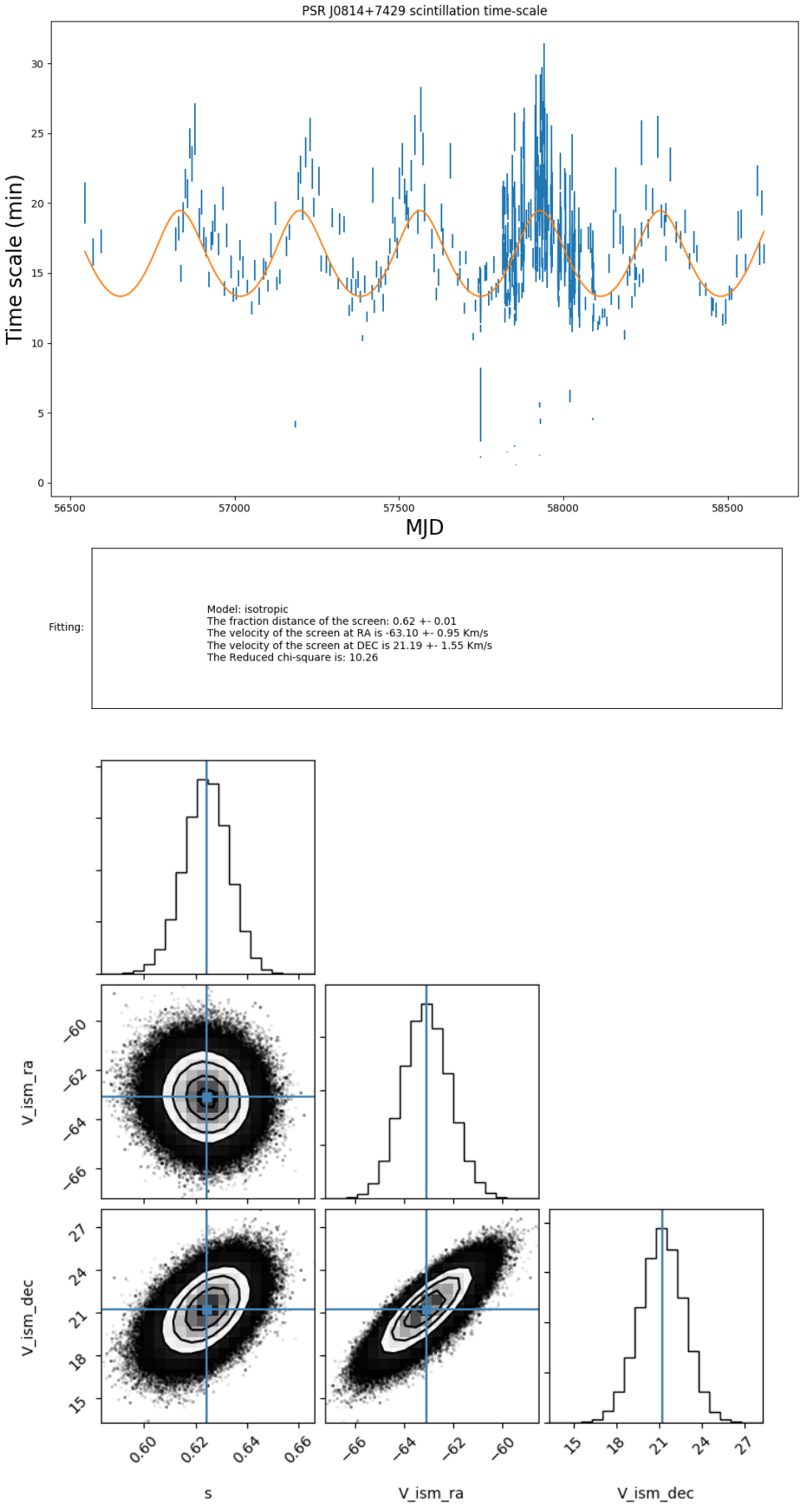

Fig. 7: Isotropic

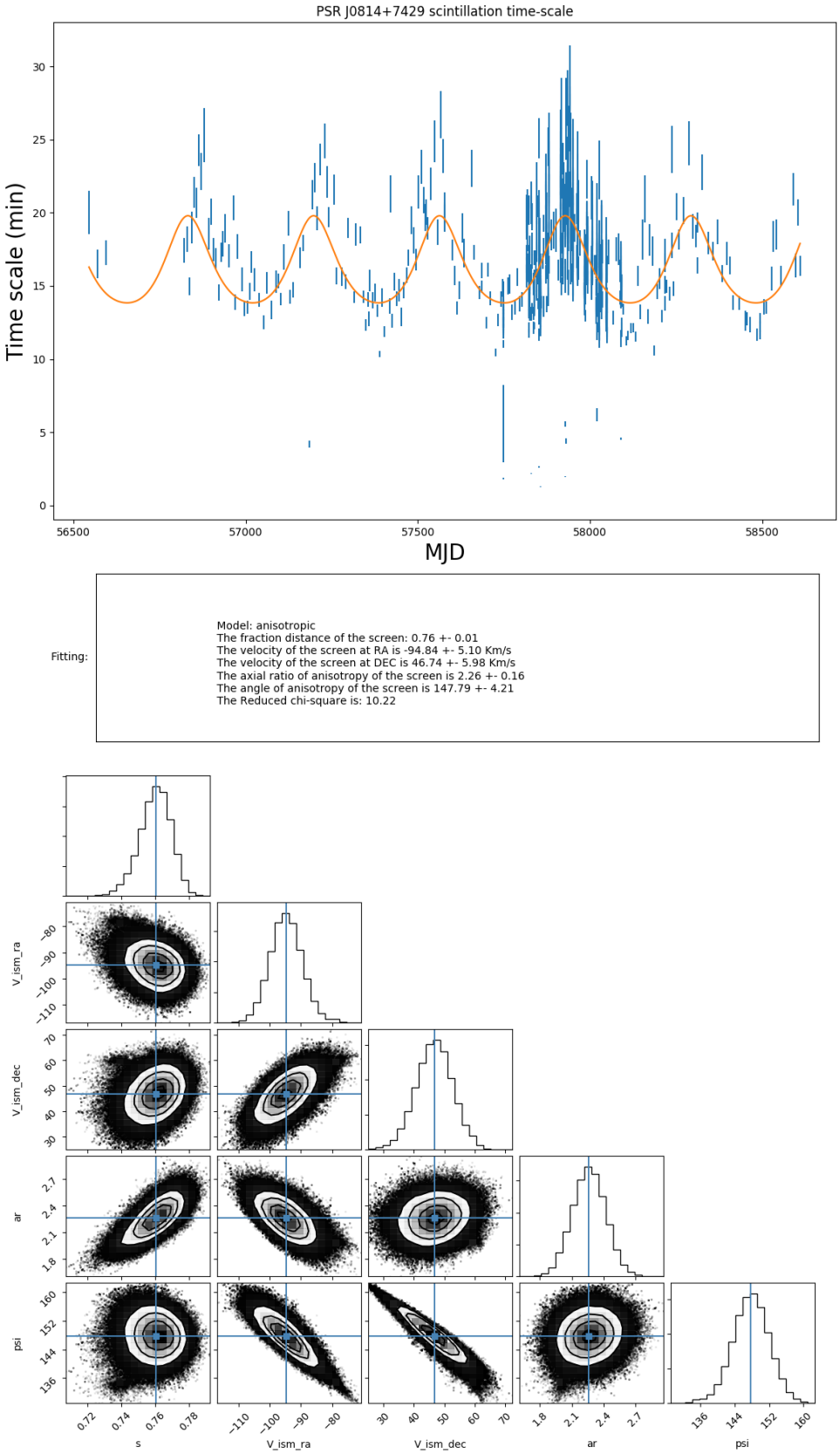

Fig. 8: anisotropic

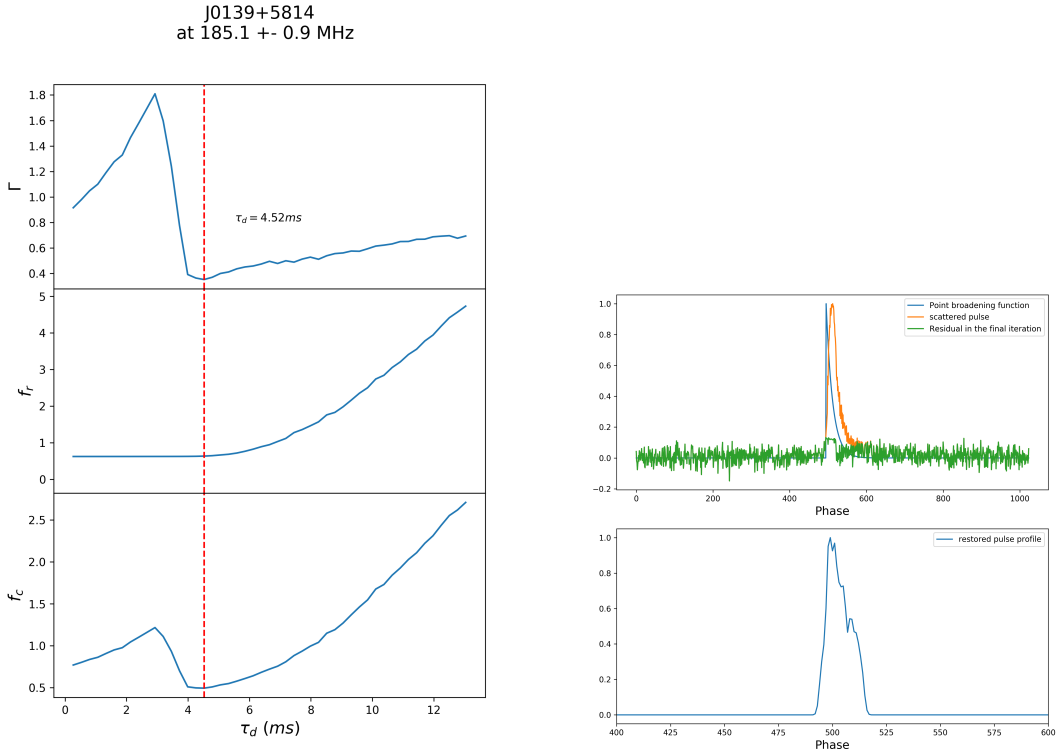

Fig. 9: Pulse broadening studies based on clean algorithm